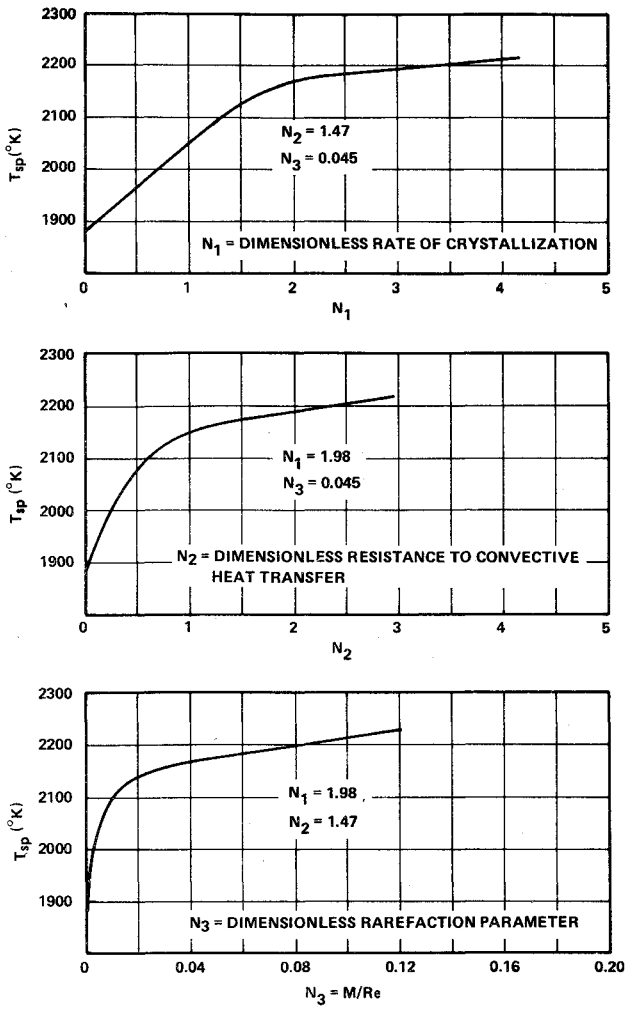

Fig. 3 Effects of dimensionless groups on spearpoint temperature.

crystallization wave speed. The relative importance of the more important parameters was determined by combining them into three dimensionless groups and determining their effect on T_{sp} by a series of parametric calculations similar to those described previously. The first of the three groups is the ratio of the time constant of the nozzle to the time constant for the kinetically limited fusion of the drop

$$N_1 = d_r \sqrt{\frac{(MW)_g}{RT_g}} \Big/ \frac{d_p}{A(T_M - T_F)^n}$$

The second group is the ratio of the time constant for convective heat transfer to the particle to the time constant of the nozzle,

$$N_2 = \frac{(d^2 \rho c)_p}{k_g} \Big/ d_r \sqrt{\frac{(MW)_g}{RT_g}}$$

The third group measures the degree of rarefaction of the flow:

$$N_3 = \frac{M}{Re} = \frac{\mu}{d_p P} \sqrt{\frac{RT}{(\gamma \cdot MW)_g}}$$

All three groups were calculated at the flow conditions corresponding to an expansion ratio of 3.5.

Results are shown in Fig. 3. Low spearpoint temperatures are associated with slow crystallization kinetics (low N_1), high convection rates (low N_2) and denser flows (low N_3). The N_3 interaction is a consequence of higher degree of convective coupling between gas and particulates at higher pressures (i.e., higher Nusselt numbers). The significant difference in spearpoint temperatures can lead to significant variations in the thermal radiation calculated from exhaust plumes.

Since accurate predictions of performance and plume radiation require knowledge of the heterogeneous crystallization velocity, experimental data on oxides other than ZrO_2 would be extremely useful.

References

[1]Turnbull, D., "Phase Changes," *Solid State Physics*, Vol. 3, Seitz, F. and Turnbull, D., eds., Academic Press, N.Y., 1956, pp. 226-310.

[2]Buckle, E.R. and Ubbelohde, A.R., "Studies on the Freezing of Pure Liquids," *Proceedings of the Royal Society*, Vol. A259, 1961, pp. 325-340, Vol. A261, 1961, pp. 189-206.

[3]Turnbull, D. and Cech, R.E., "Microscopic Observation of the Solidification of Small Metal Droplets." *Journal of Applied Physics*, Vol. 21, Aug. 1950, pp. 804-810.

[4]Thomas, D.G. and Stavely, L.A.K., "A Study of the Supercooling of Some Molecular Liquids," *Journal of the Chemical Society*, (London) 1952, pp. 4569-4577.

[5]DeNordwall, H.J. and Stavely, L.A.K., "Further Studies of the Supercooling of Drops of Some Molecular Liquids," *Journal of the Chemical Society*, (London), 1954, pp. 224-227.

[6]Atlantic Research Corporation, Alexandria, Va., QPR No. 7, "Solid Propellant Research and Development-The Study of Multiphase Flow Through Rocket Nozzles," Contract Now-61-0687-c, ARPA Order No. 22-61, Dec. 1962, pp. 83-88.

[7]Hillig, W.B. and Turnbull, D., "Theory of Crystal Growth in Undercooled Pure Liquids," *Journal of Chemical Physics*, Vol. 24, April 1956, p. 914.

[8]Rosner, D.E. and Epstein, M., "Simultaneous Kinetic and Heat Transfer Limitations in the Crystallization of Highly Undercooled Melts," *Chemical Engineering Sciences*, Vol. 30, 1975, pp. 511-520.

[9]Henderson, C.B., "Drag Coefficients of Spheres in Continuum and Rarefied Flows," *AIAA Journal*, Vol. 14, June 1976, pp. 707-708.

[10]Carlson, D.J. and Hoglund, R.F., "Particle Drag and Heat Transfer in Rocket Nozzles," *AIAA Journal*, Vol. 2, Nov. 1964, pp. 1980-1984.

Comparative Performance of Chemical Lasers with Axisymmetric and Two-Dimensional Nozzles

Harold Mirels* and Walter R. Warren, Jr.†
The Aerospace Corporation, El Segundo, California

Nomenclature

B	$= \sigma/\epsilon$
$[F]_0$	= initial atomic fluorine concentration, moles/cc
g	= local gain, $\sigma[n_u - n_l]$
I	= net local intensity
j	= 0, 1 for two-dimensional and axisymmetric nozzles, respectively
K_1	$= k_f/k_{cd}$
k_{cd}	= collisional deactivation rate (sec^{-1})
k_f	= forward pumping rate (sec^{-1})
N	= 1/2, 1 for laminar and turbulent mixing, respectively
P	= output power up to station x, Eq. (2a)
$\bar{P}$	= normalized output power up to station x, Eq. (2b)
$\bar{P}_e(j,N)$	= normalized net laser output power
p	= static pressure at nozzle exit

Received Nov. 9, 1976.
Index category: Lasers.

*Head, Aerodynamics and Heat Transfer Department, Fellow AIAA.
†Director, Aerophysics Laboratory, Associate Fellow AIAA.

R, R_0 = $r_f(x)/w$, $r_f(x_0)/w$
r = radial ordinate, Fig. 2
$r_f(x)$ = flame sheet location, Fig. 2
u = streamwise velocity
w = nozzle exit semiwidth, Fig. 1
x, x_0 = streamwise distance, Fig. 2
x_D = characteristic diffusion distance, Fig. 2
ϵ = energy per mole of photons
ζ = normalized streamwise distance, xk_{cd}/u
ζ_D = normalized diffusion distance, $x_D k_{cd}/u$
$\zeta_e(j,N)$ = normalized length of lasing region, $x_e k_{cd}/u$
σ = cross section for stimulated emission, cm^2/mole

I. Introduction

IN continuous diffusion-type cold-reaction HF chemical lasers, H_2 is diffused into supersonic jets that contain F and a diluent such as He.[1] Analytical studies of these devices have assumed that the F/He jets are generated by two-dimensional nozzles.[2-5] It is of interest to consider configurations in which axisymmetric nozzles are used because these may permit improved laser performance. Hence, the two-dimensional chemical laser model of Ref. 4 is generalized here to include axisymmetric flow. Saturated laser output power is determined for both laminar and turbulent mixing. The performance of chemical lasers with two-dimensional and axisymmetric nozzles is then compared. Nozzle wall viscous effects are neglected.

II. Analysis

We consider both axisymmetric and two-dimensional F/He nozzles. These are illustrated in Fig. 1. H_2 is added along the perimeter of the axisymmetric nozzle and along the sides of the two-dimensional nozzle.

In the simplified model of Ref. 4, it is assumed that the reactants are premixed. However, the reaction does not begin until the rectants reach a prescribed "flame sheet" location, which is denoted by $r_f = r_f(x)$ in Fig. 2. Unless otherwise specified, the notation herein is the same as in Ref. 4. We consider a saturated laser wherein $I \to \infty$, $g \to 0$, and the output power per unit volume gI remains finite. The variation of output power, with streamwise distance, for the stream tube that enters the flame sheet at (x_0, r_0) is, from Eq. (9b) of Ref. 4,

$$(2B/\sigma k_{cd}[F]_0)gI = (1+K_1)e^{-k_f(x-x_0)/u} - 1 \tag{1}$$

Let P denote the net laser output power generated up to station x per half nozzle of unit height and per nozzle for two-dimensional and axisymmetric flows, respectively. The value of dP/dx is found by integrating the contribution of all the reacted stream tubes between $r = r_f(x)$ and $r = w$. Thus

$$\frac{dP}{dx} = (2\pi)^j \int_{r_f(x)}^{w} gIr^j dr \tag{2a}$$

where $j = 0$, 1 for the two-dimensional and axisymmetric nozzles, repectively. Let $R = r_f(x)/w$ and $R_0 = r_f(x_0)/w$. Also, introduce

$$\bar{P} = 2P/\epsilon u[F]_0 \pi^j w^{1+j} \tag{2b}$$

where $\bar{P}$ is the ratio of P to the output power that would be obtained if one photon is generated for each pair of initial F atoms. (The latter output power occurs in a saturated premixed laser in the limit $K_1 \to \infty$.) Substitution of Eq. (1) into Eq. (2) and introduction of nondimensional variables yields

$$\frac{d\bar{P}}{d\zeta} = (-1)(1+K_1)\int_0^{\zeta} e^{-K_1(\zeta-\zeta_0)} \frac{dR_0^{j+1}}{d\zeta_0} d\zeta_0 - 1 + R^{j+1} \tag{3}$$

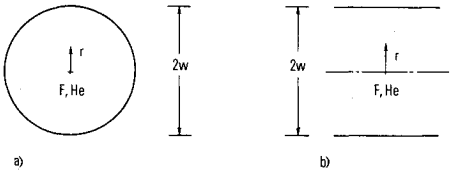

Fig. 1 Exit geometry for axisymmetric and two-dimensional F/He nozzles with characteristic diffusion distance w. a) Axisymmetric. b) Two dimensional.

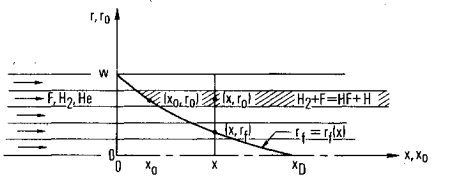

Fig. 2 Simplified mixing model.

where $\zeta = xk_{cd}/u$ is the ratio of streamwise distance x to the characteristic collisional deactivation distance u/k_{cd}. Further integration yields

$$\bar{P} = \frac{1+K_1}{K_1}\left[\int_0^{\zeta} e^{-K_1(\zeta-\zeta_0)} \frac{dR_0^{j+1}}{d\zeta_0} d\zeta_0 + 1 - R^{j+1}\right]$$

$$+ \int_0^{\zeta} R_0^{j+1} d\zeta_0 - \zeta \tag{4}$$

As ζ increases, P increases, reaches a maximum, and then decreases. The maximum value of P is denoted P_e and occurs at a station denoted ζ_e. The quantity P_e represents the saturated laser output power, and ζ_e is the length of the lasing region. ζ_e occurs at a station where $dP/d\zeta = 0$ or where $dP/d\zeta$ changes discontinuously from a positive to a negative value.

Equations (3) and (4) simplify in the limit $K_1 \to \infty$. Note that the major contribution to the integrals occurs near $\zeta = \zeta_0$. Evaluating the coefficient of $e^{-K_1(\zeta-\zeta_0)}$ at $\zeta_0 = \zeta$ in these integrals, integrating, and taking the limit $K_1 \to \infty$, we obtain

$$\frac{d\bar{P}}{d\zeta} = -dR^{j+1}/d\zeta - 1 + R^{j+1} \tag{5}$$

and

$$\bar{P} = \int_0^{\zeta} R_0^{j+1} d\zeta_0 - \zeta + 1 - R^{j+1} \tag{6}$$

These expressions can be evaluated when R is specified.

In the present study, we assume

$$R = 1 - (\zeta/\zeta_D)^N \qquad \zeta < \zeta_D \tag{7a}$$

$$= 0 \qquad \zeta > \zeta_D \tag{7b}$$

for both two-dimensional and axisymmetric nozzles. Here, $N = 1/2$, 1 for laminar and turbulent diffusion, respectively, and ζ_D is the value of ζ at which the flame sheet reaches the nozzle centerline.

It is assumed here that, for given exit flow conditions, and a given value of w, the value of ζ_D is the same for both two-dimensional and axisymmetric nozzles. For the two-dimensional nozzles, Eqs. (7) agree with the flame sheet shape used previously in Ref. 4. For the axisymmetric nozzles, the mixing is essentially two dimensional when $\zeta/\zeta_D \ll 1$. Hence, the use of Eqs. (7) with the same value of ζ_D for both two-dimensional and axisymmetric nozzles is clearly valid when $\zeta_e/\zeta_D \ll 1$. As ζ/ζ_D increases, the rate at which H_2 diffuses into the F/He stream tends to be more rapid for the

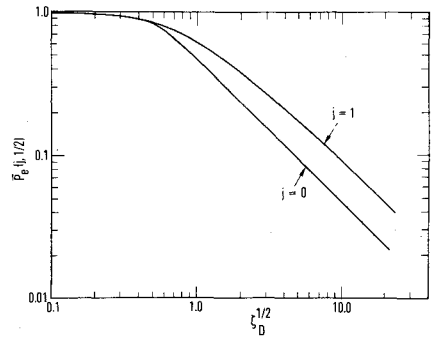

Fig. 3 Variation of output power $\bar{P}_e(j, 1/2)$ with diffusion rate parameter $\zeta_D^{1/2}$ for laminar flow and $K_I \to \infty$.

axisymmetric than for the two-dimensional nozzle because of transverse curvature effects. This feature of the mixing process is not modeled here.

For simplicity, we obtain closed-form results for $K_I \to \infty$, although similar closed-form expressions can be obtained for finite values of K_I. In order to display the dependence of the dependent variables on j and N, we introduce the notation $\zeta_e(j,N)$, $\bar{P}_e(j,N)$.‡

The quantity $\zeta_e(j,N)$ is found by setting Eq. (5) equal to zero or observing the value of ζ at which $dP/d\zeta$ changes discontinuously from a positive to a negative value. This procedure yields

$$\zeta_e(0,N) = N \qquad \zeta_D > N \tag{8a}$$

$$= \zeta_D \qquad \zeta_D < N \tag{8b}$$

$$\zeta_e(1,1/2) = (1/2)[1 - (\zeta_e/\zeta_D)^{1/2}(1-\zeta_e)] \tag{8c}$$

$$= \zeta_D\{1 - \zeta_e[2 - (\zeta_e/\zeta_D)^{1/2}]\}^2 \tag{8d}$$

$$\zeta_e(1,1) = 1 + \zeta_D - (1+\zeta_D^2)^{1/2} \tag{8e}$$

Equations (8c) and (8d) are solved by iteration, with Eq. (8c) used for $\zeta_D > 1/2$ and Eq. (8d) for $\zeta_D < 1/2$. Initial estimates are $\zeta_e = 1/2$ in Eq. (8c) and $\zeta_e = \zeta_D$ in Eq. (8d). Except for Eq. (8b), the above expressions correspond to stations where $dP/d\zeta = 0$ and $\zeta_e/\zeta_D < 1$. For these cases, lasing terminates before the flame sheet reaches the nozzle centerline. Equation (8b) corresponds to the case in which lasing is terminated by the arrival of the flame sheet at the nozzle centerline. The corresponding laser output power is

$$\bar{P}_e(0,N) = (N/\zeta_D)^N/(N+1) \qquad \zeta_D > N \tag{9a}$$

$$= 1 - \zeta_D/(N+1) \qquad \zeta_D < N \tag{9b}$$

$$\bar{P}_e(1,N) = 2\left(\frac{\zeta_e}{\zeta_D}\right)^N\left[1 - \frac{\zeta_e}{N+1}\right] - \left(\frac{\zeta_e}{\zeta_D}\right)^{2N}\left[1 - \frac{\zeta_e}{2N+1}\right] \tag{9c}$$

For given values of ζ_D and N, Eq. (9c) can be evaluated by substituting the value of ζ_e obtained from Eqs. (8c), (8d), or (8e). In the limit $\zeta_D^N \gg 1$, Eqs. (8) and (9) indicate

$$\zeta_e(1,N) = N\left[1 - \frac{1}{2}\left(\frac{N}{\zeta_D}\right)^N + O\left(\frac{N}{\zeta_D}\right)^{4N-1}\right] \tag{10a}$$

$$\bar{P}_e(1,N) = \frac{2}{N+1}\left(\frac{N}{\zeta_D}\right)^N\left[1 - \frac{(N+1)^2}{2(2N+1)}\left(\frac{N}{\zeta_D}\right)^N + O\left(\frac{N}{\zeta_D}\right)^{2N}\right] \tag{10b}$$

These equations provide, explicitly, the dependence of $\zeta_e(1,N)$ and $\bar{P}_e(1,N)$ on ζ_D for ζ_D large.

Equations (8) and (9) have been evaluated numerically and the results are presented in Table 1. The variation of $\bar{P}_e(j, 1/2)$ with $\zeta_D^{1/2}$ is indicated in Fig. 3. The quantity $\bar{P}_e(0,N)/\bar{P}_e(1,N)$ in Table 1 can be interpreted as the ratio of two-dimensional to axisymmetric nozzle output power for cases where both nozzles have the same exit flow conditions and the same semiwidth w. For small values of ζ_D^N, both nozzles have the same output power. In these cases, the diffusion is fast, relative to the deactivation, and the performance is similar to that for a premixed laser. For ζ_D^N large, the two-dimensional nozzle has one-half the output power of the axisymmetric nozzle because only the small portion of the F/He stream in direct contact with the bounding H_2 stream lases. Since the "wetted perimeter" is twice as large for the axisymmetric as for the two-dimensional nozzle, the output power from the former is twice as great as that from the latter. The output power, however, is relatively low in this region. The ratio of two-dimensional to axisymmetric output power is slightly larger than 1 for values of ζ_D^N between 0.1 and 1.0. This is probably because the same flame sheet shape was assumed for corresponding axisymmetric and two-dimensional flows. In reality, the axisymmetric diffusion rate is faster than the two-dimensional diffusion rate, which should cause the ratio of two-dimensional to axisymmetric output power to be ≤ 1 for all ζ_D^N. Both the two-dimensional and the axisymmetric nozzles have similar performance in the region $0.1 \leq \zeta_D^N \leq 1.0$, hence a more accurate description of the diffusion process appears unwarranted, particularly for laminar diffusion, which is the case of primary interest.

Table 1 Output power $\bar{P}_e$ and length of lasing region ζ_e for $K_I \to \infty$

ζ_D^N	j = 0				j = 1				$\bar{P}_e(0,N)/\bar{P}_e(1,N)$	
	N = 1/2		N = 1		N = 1/2		N = 1			
	$\bar{P}_e$	ζ_e	$\bar{P}_e$	ζ_e	$\bar{P}_e$	ζ_e	$\bar{P}_e$	ζ_e	N = 1/2	N = 1
0.1	0.993	0.01	0.950	0.1	0.992	0.010	0.936	0.095	1.001	1.015
0.2	0.973	0.04	0.900	0.2	0.968	0.037	0.877	0.180	1.005	1.026
0.4	0.893	0.16	0.800	0.4	0.888	0.120	0.772	0.323	1.006	1.036
0.6	0.760	0.36	0.700	0.6	0.792	0.201	0.685	0.434	0.960	1.022
0.8	0.589	0.50	0.600	0.8	0.700	0.264	0.613	0.519	0.841	0.979
1.0	0.471	0.50	0.500	1.00	0.622	0.308	0.552	0.586	0.757	0.906
2.0	0.236	0.50	0.250	1.00	0.384	0.405	0.363	0.764	0.614	0.689
4.0	0.118	0.50	0.125	1.00	0.213	0.454	0.212	0.877	0.554	0.590
6.0	0.079	0.50	0.083	1.00	0.147	0.470	0.149	0.917	0.537	0.557
8.0	0.059	0.50	0.0625	1.00	0.112	0.477	0.115	0.938	0.527	0.543
10.0	0.047	0.50	0.050	1.00	0.091	0.482	0.094	0.950	0.516	0.555
20.00	0.024	0.50	0.025	1.00	0.046	0.491	0.048	0.975	0.522	0.521

III. Concluding Remarks

Approximate expressions for ζ_D^N are given by Eqs. (44) of Ref. 4. For a HF laser with laminar flows and a helium diluent

$$\zeta_D^{1/2} = 3.27 \frac{p(\text{Torr})w(\text{cm})}{(p/p_F)^{1/2}} \left[\frac{2}{A} \left(\frac{400}{T} \right)^{1.385} \right] \tag{11a}$$

where p is the static pressure, and p_F is the partial pressure of the fluorine at the nozzle exit. Equation (11a) neglects the effect of combustion-generated deactivators. For typical flow conditions ($p/p_F = 10$, $T = 400\,K$, $A = 2$)

$$\zeta_D^{1/2} = p(\text{Torr})w(\text{cm}) \tag{11b}$$

For this flow condition, a saturated laser, $K_I \to \infty$, and $pw > 5$ Torr cm, i.e., $\zeta_D^{1/2} > 5$, the axisymmetric nozzle has an output power twice that of a two-dimensional nozzle with the same exit flow conditions and exit width w. In this pw regime, however, the chemical efficiency of the axisymmetric nozzle is 20% or less that of a premixed ($pw = 0$) laser. For $pw = 1$ Torr cm, i.e., $\zeta_D^{1/2} = 1$, the axisymmetric nozzle has about 30% greater output than the corresponding two-dimensional nozzle and a chemical efficiency equal to about 60% that of a premixed laser. For $pw < 0.5$ Torr cm, i.e., $\zeta_D^{1/2} < 0.5$, both nozzles have essentially premixed laser performance. For either nozzle, a reduction in pw results in improved performance (Fig. 3). The effect of $p/p_F \neq 10$ is found in Eq. (11a).

Fabrication and nozzle wall boundary-layer effects also have to be considered when comparing two-dimensional and axisymmetric nozzles. These are beyond the scope of this study.

Acknowledgment

The present study was supported by NAVSEA HEL project PMS-405 through U.S. Air Force Space and Missile System Organization (SAMSO) Contract No. F04701-75-C-0076.

References

[1]Spencer, D. J., Mirels, H., and Durran, D. A., "Performance of CW HF Chemical Laser with N_2 or He Diluent," *Journal of Applied Physics*, Vol. 43, March 1972, p. 1151.

[2]Hofland, R. and Mirels, H., "Flame Sheet Analyses of CW Diffusion-Type Chemical Lasers, I. Uncoupled Radiation," *AIAA Journal*, Vol. 10, April 1972, pp. 420-428.

[3]Hofland, R. and Mirels, H., "Flame Sheet Analyses of CW Diffusion-Type Chemical Lasers, II. Coupled Radiation," *AIAA Journal*, Vol. 10, Oct. 1972, pp. 1271-1280.

[4]Mirels, H., Hofland, R., and King, W. S., "Simplified Model CW Diffusion-Type Chemical Lasers," *AIAA Journal*, Vol. 11, Feb. 1973, pp. 156-164.

[5]Broadwell, J. E., "Effect of Mixing Rate on HF Chemical Laser Performance," *Applied Optics*, Vol. 13, April 1974, p. 962.

Review of Wind-Tunnel Freestream Pressure Fluctuations

A.J. Laderman*
Ford Aerospace & Communications Corporation, Newport Beach, Calif.

Nomenclature

c_f	= skin friction coefficient
D	= diameter or height of tunnel test section
M	= Mach number
p	= pressure
$Re_{\infty,D}$	= freestream Reynolds number based on tunnel diameter
δ^*	= boundary-layer displacement thickness
γ	= specific heat ratio
τ_w	= wall shear stress
$()'$	= fluctuating quantity
$<()'>$	= rms value
$(\bar{})$	= mean value
Subscripts	
∞	= freestream condition
c	= model surface condition

Received Dec. 31, 1976.

Index categories: Supersonic and Hypersonic Flow; Nozzle and Channel Flow.

*Principal Scientist, Fluid Mechanics Department. Member AIAA.

IT is commonly agreed that pressure fluctuations in the freestream of supersonic-hypersonic wind tunnels have a strong influence on boundary-layer transition over aerodynamic models. The pressure fluctuations arise from interaction between the turbulent boundary layer growing on the tunnel sidewalls and the freestream flow, and it is known that the fluctuations become large for $M_\infty \geq 2.5$. In fact, for unheated tunnels with $M_\infty > 3$ the pressure fluctuations completely dominate the freestream disturbance modes. In heated wing tunnels where the other modes, particularly the entropy mode, become active, the pressure fluctuations still represent a significant portion of the total disturbance level and they increase in importance as M_∞ increases. Over a dozen measurements of freestream pressure fluctuations, obtained with both hot wire anemometers and acoustical transducers in a variety of facilities, have been reported.[1-12] So far, attempts to predict freestream noise, which were generally based on theories of sound radiated from a turbulent boundary layer (Refs. 13 and 14), have not been fruitful. On the other hand, several years ago Pate and Schuller[9] demonstrated a relation between transition Reynolds number on wind-tunnel models and radiated pressure disturbances. On the basis of these measurements they were successful in correlating the transition Reynolds number for a large number of wind-tunnel facilities with the parameters believed also to influence sound generation by the turbulent sidewall boundary layer, including wall shear stress, displacement thickness, tunnel size, etc. More recently, Stainback and Rainey[15] presented a correlation for freestream pressure fluctuations in terms of similar parameters. However, while their correlation provided a reasonable fit to most of the data upon which it is based, they treated hot wire data and acoustic measurements separately. More important, they omitted the acoustical measurements of Pate and Schuller[9] and of Dougherty[12] which, as described later, show a marked departure from the behavior exhibited by the bulk of the reported data. This paper presents a further review of the freestream pressure fluctuations and serves to illustrate the significant trends which characterize the existing measurements.

Measurement of freestream pressure fluctuations has been made using either the hot wire anemometer or acoustical transducers (the latter have been mounted flush with the surface of a sharp cone or flat plate and measurements made for conditions producing laminar boundary-layer flow over the model). The measurements considered in this Note are listed in Table 1. The hot wire measurements of Stainback et al.[7] at high hypersonic Mach numbers ($M_\infty \sim 15$ to 20) showed that the ratio $<p'>/\bar{p}$ remains constant across weak oblique shock waves, i.e., that $<p'>/\bar{p}_\infty = <p_c'>/\bar{p}_c$. This suggested, therefore, that acoustic measurements of fluctuating surface pressure could be used to determine the freestream pressure disturbances and, in fact, early measurements by NASA Langley researchers[7] indicated that acoustical measurements of $<p_c'>/\bar{p}_c$ were in accord with hot wire measurements of $<p_\infty'>/\bar{p}_\infty$. However, more recently, the Langley group concluded that acoustic